Mol Neurobiol
DOI 10.1007/s12035-015-9263-6

Attenuated Reactive Gliosis and Enhanced Functional Recovery Following Spinal Cord Injury in Null Mutant Mice of Platelet-Activating Factor Receptor

Yuanyi Wang[1,2] · Zhongwen Gao[2,5] · Yiping Zhang[3] · Shi-Qing Feng[2,4] · Yulong Liu[2,5] · Lisa B. E. Shields[3] · Ying-Zheng Zhao[2,6] · Qingsan Zhu[5] · David Gozal[7] · Christopher B. Shields[3,8] · Jun Cai[2,8]

Received: 12 January 2015 / Accepted: 28 May 2015

Abstract Platelet-activating factor (PAF) is a unique phosphoglycerine that mediates the biological functions of both immune and nervous systems. Excessive PAF plays an important role in neural injury via its specific receptor (PAFR). In this study, we hypothesized that PAF signaling activates reactive gliosis after spinal cord injury (SCI), and blocking the PAF pathway would modify the glia scar formation and promote functional recovery. PAF microinjected into the normal wild-type spinal cord induced a dose-dependent activation of microglia and astrocytes. In the SCI mice, *PAFR* null mutant mice showed a better functional recovery in grip and rotarod performances than wild-type mice. Although both microglia and astrocytes were activated after SCI in wild-type and *PAFR* null mutant mice, expressions of IL-6, vimentin, nestin, and GFAP were not significantly elevated in *PAFR* null mutants. Disruption of PAF signaling inhibited the expressions of proteoglycan CS56 and neurocan (CSPG3). Intriguingly, compared to the wild-type SCI mice, less axonal retraction/dieback at 7 dpi but more NFH-labeled axons at 28 dpi was found in the area adjacent to the epicenter in *PAFR* null mutant SCI mice. Moreover, treatment with PAFR antagonist Ginkgolide B (GB) at the chronic phase rather than acute phase enhanced the functional recovery in the wild-type SCI mice. These findings suggest that PAF signaling participates in reactive gliosis after SCI, and blocking of this signaling enhances functional recovery and to some extent may promote axon regrowth.

Keywords Glial scar · Astrocyte · Axon regeneration · Spinal cord injury · Dorsal laceration

Introduction

Reactive gliosis, also known as glial scar (GS) formation, is an inflammatory response mainly characterized by the proliferation of microglia and astrocytes as well as astrocytic hypertrophy occurring after injury in the central nervous system

Yuanyi Wang, Zhongwen Gao and Yiping Zhang contributed equally to this work.

✉ Qingsan Zhu
drzqs@yahoo.com.cn

✉ Jun Cai
j0cai002@louisville.edu

[1] Department of Spine Surgery, First Hospital of Jilin University, 71 Xinmin Street, Changchun, Jilin 130021, People's Republic of China

[2] Department of Pediatrics, University of Louisville School of Medicine, 570 S. Preston Street, Donald Baxter Building, Suite 321B, Louisville, KY 40202, USA

[3] Norton Healthcare, Norton Neuroscience Institute, Louisville, KY 40202, USA

[4] Department of Orthopedics, General Hospital of Tianjin Medical University, Tianjin 300052, People's Republic of China

[5] Department of Orthopedics, China-Japan Union Hospital of Jilin University, Changchun 130033, People's Republic of China

[6] Pharmacy School, Wenzhou Medical University, Wenzhou 325035, People's Republic of China

[7] Comer Children's Hospital, Department of Pediatrics, University of Chicago, Chicago, IL 60637, USA

[8] Department of Anatomical Sciences and Neurobiology, University of Louisville School of Medicine, Louisville, KY 40202, USA

Published online: 18 June 2015

(CNS). The GS consists predominately of activated microglia/macrophages, reactive astrocytes, and extracellular matrix (ECM) molecules (e.g., proteoglycans) with invading connective tissue components. Glial scarring is triggered by molecules and cells from the vasculature crossing breaches in the blood-brain or blood-cord barrier (BBB or BCB) into the CNS [1], which results in the activation of microglia/macrophage and astrocyte. The GS plays an important role in both beneficial and detrimental effects on injury recovery. It isolates the injured site from adjacent normal tissue to prevent further inflammatory damage and reestablishes the integrity of the CNS by forming physical and molecular barriers [2, 3] which may provide mechanical support, blood flow modulation, BBB/BCB repair, anti-inflammatory molecules, and neuronal/oligodendroglial protection from the excitotoxicity. Meanwhile, reactive astrocytes with increased synthesis of intermediate filaments such as GFAP and vimentin can release inhibitory proteoglycans (e.g., CSPGs and KSPGs) to drive back axon regeneration [4] and inhibit the remyelinating process of oligodendrocytes [5]. In addition, activated microglia and/or astrocytes also produce excitotoxic glutamate and neurotoxic substances including pro-inflammatory and cytotoxic cytokines [6]. However, the molecular triggers of reactive gliosis, including microgliosis and astrogliosis, remain poorly understood.

Platelet-activating factor (PAF, 1-alkyl-2-acetyl-sn-glycero-3-phosphocholine) is a unique phosphoglycerine that mediates the biological functions of both immune and nervous systems. It is released by a wide variety of cells, such as platelets, macrophages, neutrophils, endothelial cells, mast cells, and neural cells, and exerts its biological effects via ubiquitously distributed G-protein coupled PAF receptor [7]. PAF can be synthesized within cellular membranes via two pathways—de novo metabolic pathway and cytosolic phospholipase A_2 ($cPLA_2$)-dependent remodeling pathway, which are believed to maintain physiological functions or cause pathological responses, respectively [8]. In the CNS, neurons and glial cells can synthesize PAF at a lower level [9, 10], and platelet-activating factor receptor (PAFR) has been identified in neuron, microglia, astrocyte, and oligodendrocyte progenitor cell [11–14]. Excessive PAF appears to play an important role in neural injury, such as ischemia-reperfusion injury, stroke, inflammation, HIV-induced neurotoxicity, meningitis, cognitive deficits, and multiple sclerosis [15–18]. It has been reported that $cPLA_2$ expression and PAF level were dramatically elevated after the spinal cord injury (SCI) [19–22], and PAF antagonist pretreatment reduced messenger RNA (mRNA) of pro-inflammatory cytokines IL-1α/β and IL-6 in the acute phase of injury [18]. Nevertheless, it has not been identified whether PAF signaling is involved in modeling the GS formation and functional changes after SCI.

In the present study, we tested our hypothesis that PAF signaling activates the reactive gliosis after SCI, and blocking of the PAF pathway would modify GS formation and enhance neurobehavioral performance. The findings showed that disruption of PAF signaling via *PAFR* deletion or antagonist administration inhibited activation of microglia and astrocytes leading to extracellular matrix (ECM) remodeling and promoted axonal regeneration and functional recovery.

Materials and Methods

Experimental Animals

C57BL/6 wild-type (Jackson Laboratory, Bar Harbor, ME) and *PAFR* null mutant mice (kindly provided by Dr. Nicholas Bazan) were bred onsite. Genotyping of *PAFR* conventional knockout mice was performed as previously reported procedures [23]. Six- to 8-week-old wild-type C57BL/6 and *PAFR*−/− female mice were housed with diet and water available ad libitum in an animal facility and maintained in a temperature- and light-controlled environment with an alternating 12-h light/dark cycle. All procedures were supervised by the University of Louisville Research Resources Center, an AALAC approved facility and performed in accordance with the guidelines of the Animal Care and Use Committee of University of Louisville School of Medicine and NIH requirements for care and use of laboratory animals. After surgery, mice were housed in a clean cage. Lactated Ringer's solution (1.5 ml), buprenorphine (2.0 mg/kg body weight), and antibiotic (gentamicin, 10 mg/kg body weight) were administered subcutaneously twice a day for 72 h. Water and soft diet were easily reached.

Intraspinal Injection of PAF

Twelve wild-type female mice were randomly assigned for four experimental groups—two vehicle groups, low-dose PAF injection group, and high-dose PAF injection group (three mice per group). The mice were deeply anesthetized with avertin (400 mg/kg body weight, Sigma) via peritoneal injection. The C4–C7 dorsal spinal segments were exposed, and the spinal column was stabilized. The microinjections (two shots/side, 0.5 or 1 μl/shot) with PAF (0.04 ng/μl, Sigma-Aldrich) were made into the right side and vehicle (1×PBS containing DMSO) into the left side at 0.5 mm from the midline at the C5–C6 spinal level with a depth of 1.3 and 0.8 mm from the dorsal cord surface using a glass micropipette attached to a Hamilton syringe (Hamilton Company, Reno, NV, USA). The fixed C5–C6 spinal segments were collected at 5 dpi.

Dorsal Laceration SCI

Eighty-six wild-type or *PAFR* null mutant female mice were randomly divided into sham (n=38) and SCI (n=48, ~25 % mortality plus humane endpoints after SCI) groups, respectively. The C4–C7 dorsal spinal segments were exposed, and the spinal column was stabilized in the deeply anesthetized mouse. After the dura was punctured at the C5–C6 spinal level using a sterile 30-gauge needle, a precise dorsal hemisection with a 0.75-mm depth and 1.00-mm width was conducted using a VibraKnife [24, 25]. For sham control mice, only the dural was punctured at the C5–C6 spinal level. Three fresh and three fixed C5–C6 spinal segments were collected from 30 mice per group at 3, 7, 14, 21, and 28 dpi, respectively. Eight sham mice and 12 SCI mice were randomly selected after surgery for grip and rotarod tests until euthanasia at 42 dpi for tissue collection.

Grip Test for Forelimb Strength

A low-force testing system (ALMEMO, Woodland Hills, CA, USA) was used to measure the forelimb grip strength of mice by a force transducer equipped with a metal bar (length 16 cm, diameter 1 mm). On the test day, two trials with an interval of 1 h were applied on each mouse. The mouse was allowed to grab the metal bar and was gently pulled by its tail to keep its body in a horizontal position and both forelimbs straight. The horizontal pulling force was gradually increased until the mouse released its claws from the bar. The test was repeated three times, and the maximum forelimb strength (gram) was considered as the result. The average value of two trials was recorded as the grip score. The test was performed at −1 (baseline recording), 3, 7, 14, 21, 28, 35, and 42 dpi. To avoid the functional variation between different mice, the percentage of the individual grip strength to its baseline was used to assess functional recovery. The valid data of forelimb grip strength that ruled out the measurements discontinued due to death or humane endpoint that was eventually collected from the following mice: (1) wild-type sham mice (n=8), (2) PAFR−/− sham mice (n=5), (3) wild-type SCI mice (n=10), and (4) *PAFR*−/− SCI mice (n=8). Data acquisition and analysis were performed with experimenter blinding.

Rotarod Performance

This test assessed neural functions on balance, coordination, and sensorimotor and motor planning. A 2-day training/test regimen was adopted for mice running on the rotarod (UgoBasile 7650 accelerating RotaRod, Varese, Italy.) with an accelerating speed from 4 to 40 rpm in 600 s [26, 27]. One trial was recorded from the time the rotarod began running until the mouse fell off. Three trials with an interval of 1 h were conducted on each mouse either for training or testing. The average running time of three trials was recorded as the rotarod score. The test was performed at −1 (baseline recording), 3, 7, 14, 21, 28, 35, and 42 dpi. To avoid the functional variation between different mice, the percentage of the individual rotarod score to its baseline score was used to assess the functional recovery. The following mice were eventually tested for performance evaluation: (1) wild-type sham mice (n=8), (2) *PAFR*−/− sham mice (n=5), (3) wild-type SCI mice (n=10), and (4) *PAFR*−/− SCI mice (n=8). Data acquisition and analysis were performed with experimenter blinding.

Tissue Collection and Cryostat Sectioning

The C5–C6 spinal segment was dissected for fresh tissue collection in liquid nitrogen after cardiac perfusion with saline or for fixed tissue collection following cardiac perfusion with 4 % paraformaldehyde. The fixed spinal segment was submerged in 4 % PFA at 4 °C overnight, followed by 30 % sucrose in PBS overnight, and then embedded in OCT media. The serial transverse or sagittal sections (16 μm) were collected on a cryostat.

Immunofluorescence Staining

Single or double immunofluorescence on cryostat spinal sections was performed as described previously [28, 29]. The images were captured using an epifluorescence microscope (Nikon Eclipse E800). Antibodies were commercially available. The dilution ratio of antibodies is as follows: rat anti-CD68 (1:50, Biolegend, San Diego, CA, USA), mouse anti-nestin (1:100, Millipore, Billerica, MA, USA), rabbit anti-GFAP (1:500, Dako, Carpinteria, CA, USA), mouse anti-chondroitin sulfate (anti-CS, 1:200, Sigma, St. Louis, MO, USA), mouse anti-NF200 (1:1000, Abcam, Cambridge, MA, USA), and mouse anti-phospho-NF200 (1:1000, Abcam).

For quantitative analysis, $CD68^+$ cell numbers in the spinal cord were counted and expressed as number of cells per square millimeter based on the section area outlines in ImageJ. Percentage of GFAP/nestin- or CS-immunoreactive area normalized to the total image area was calculated. The volume of gliosis in the SCI mice was estimated by outlining the core area adjacent to lesion epicenter with GFAP/nestin staining multiplied by total thickness of sections for each animal. The analyzer was blinded to the experimental condition during counting and image analysis.

Western Blotting

Protein samples were prepared from C5 and C6 spinal segments in CelLytic™ MT Cell Lysis Reagent (Sigma) plus Complete Protease Inhibitors (Roche, Nutley, NJ, USA) at 4 °C. Equivalent total protein amounts were loaded onto 7

or 10 % polyacrylamide gels (Bio-Rad, Hercules, CA, USA) and then transferred to Protan BA83 Nitrocellulose Membranes (Midwest Scientific, St. Louis, MO, USA) as previously described [30]. Blots were probed and recognized with the following first and second antibodies: rabbit anti-Iba1 (1:2000, Wako, Richmond, VA, USA), rabbit anti-IL-6 (1:3000, Millipore), mouse anti-GFAP (1:4000, Cell Signaling, Beverly, MA, USA), mouse anti-vimentin (1:4000, Sigma), mouse anti-neurocan (1:5000, Sigma), mouse anti-NF200 (1:3000, Abcam), mouse anti-phospho-NF200 (1:1000, Abcam), anti-β-actin (1:5000, Sigma), anti-β-tubulin (1:5000, Sigma), and HRP-linked goat-anti-mouse or anti-rabbit (Jackson Immunology, West Grove, PA, USA). Signals were developed by using chemiluminescence with ECL Western blotting detection reagent (Pierce, Rockford, IL, USA) and exposed to film. The optical density (OD) of bands on Western blot was measured using the NIH ImageJ software. The ODs for specific protein were normalized over the ODs for β-tubulin or β-actin, and these values were expressed as the ratio relative to the control.

Treatment with PAFR Competitive Antagonist

Ginkgolide B (GB, Selleckchem, Houston, TX, USA) dissolved in 1× PBS containing 50 % DMSO or 1× PBS containing 50 % DMSO alone as control was injected subcutaneously (100 mg/kg body weight) once a day in 44 wild-type female mice, and the valid measurements were collected from the following mice: (1) wild-type mice with 1× PBS containing 50 % DMSO for 42 days (n=4), (2) wild-type mice with GB in 1× PBS with 50 % DMSO for 42 days (n=4), (3) wild-type SCI mice with 1× PBS containing 50 % DMSO from 1 to 42 dpi (n=10), (4) wild-type mice with GB from 1 to 10 dpi followed by 1× PBS containing 50 % DMSO until 42 dpi (acute phase, n=12), and (5) wild-type SCI mice with 1× PBS containing 50 % DMSO from 1 to 10 dpi followed by GB until 42 dpi (subacute and chronic phases, n=7).

Statistical Analysis

The statistical analysis was performed using SPSS 22 for Windows. Data were presented as mean±SD values for normally distributed variables. One-way analysis of variance (ANOVA) with repeated measures was applied to compare the body weight between wild-type and *PAFR*−/− null mutant mice during the postnatal development. The comparisons of treatments (sham vs. SCI) in mice with different genotypes (wild-type vs. *PAFR*−/−) were performed at the same time periods of treatment using two-way repeated measures ANOVA with Bonferroni post hoc tests. For GB administration, the comparisons of treatments (vehicle vs. GB) in wild-type or wild-type SCI mice were conducted at the same time periods of treatment using one-way repeated measures ANOVA with Bonferroni post hoc tests. Data from immunofluorescent staining and Western blot were analyzed using one-way ANOVA with Newman-Keuls post hoc tests. The significant level was considered $p<0.05$.

Results

Normal Development of Gross Growth, Microglia, and Astrocytes in *PAFR* Null Mutant Mice

PAFR null mutant mice possess normal reproductivity without gross malformation in the brain [23]. Further examination in this study showed that postnatal body weight and locomotor function in the adult were not statistically different between *PAFR*−/− and wild-type mice (Figs. 1a and 3). In neonatal null mutant spinal cords at P6, expression of Iba1 but not GFAP was significantly lower than that in wild-type ones, suggesting that PAF signal may be required for microglia development. In young adult null mutant mice, Iba1$^+$ resting/surveying microglia and GFAP$^+$ astrocytes in the spinal cord did not show any change in either cellular morphology or cell numbers (Fig. 1b, data not shown).

Dose-Dependent Activation of Microglia and Astrocytes by Exogenous PAF In Vivo

It has been reported that PAF level is elevated by approximately 13- to 20-fold in the injured spinal cord [19, 22]. To assess whether excessive PAF would activate microglia and astrocytes, PAF (0.04 or 0.08 ng) and vehicle solution were microinjected into one side of normal wild-type spinal cords. As expected, only a few CD68$^+$ microglia (Fig. 2a, b) and GFAP$^+$/nestin$^+$ astrocytes (Fig. 2d, e) were found on the side in which the vehicle was injected. In contrast, many more microglia and astrocytes were activated and confined to the surrounding area at the site of injection with PAF in a dose-dependent manner (Fig. 2c, f), which resulted in a significantly larger lesion core volume (Fig. 2g).

Functional Improvement in *PAFR* Null Mutant Mice After Cervical SCI

Previous studies showed that *PAFR* knockout mice possess significantly milder response to anaphylaxis and inflammation than wild-type mice [23], and PAF antagonist pretreatment reduced mRNA of pro-inflammatory cytokines IL-1α/β and IL-6 in the acute phase of injury [18]. Thus, we assumed that the functional recovery in *PAFR*−/− mutants would vary from that in wild-type mice after SCI possibly due to their differences in immune response. To test this hypothesis, we conducted a precise dorsal hemisection between the C5 and C6 spinous processes in mice by use of the VibraKnife, which cut

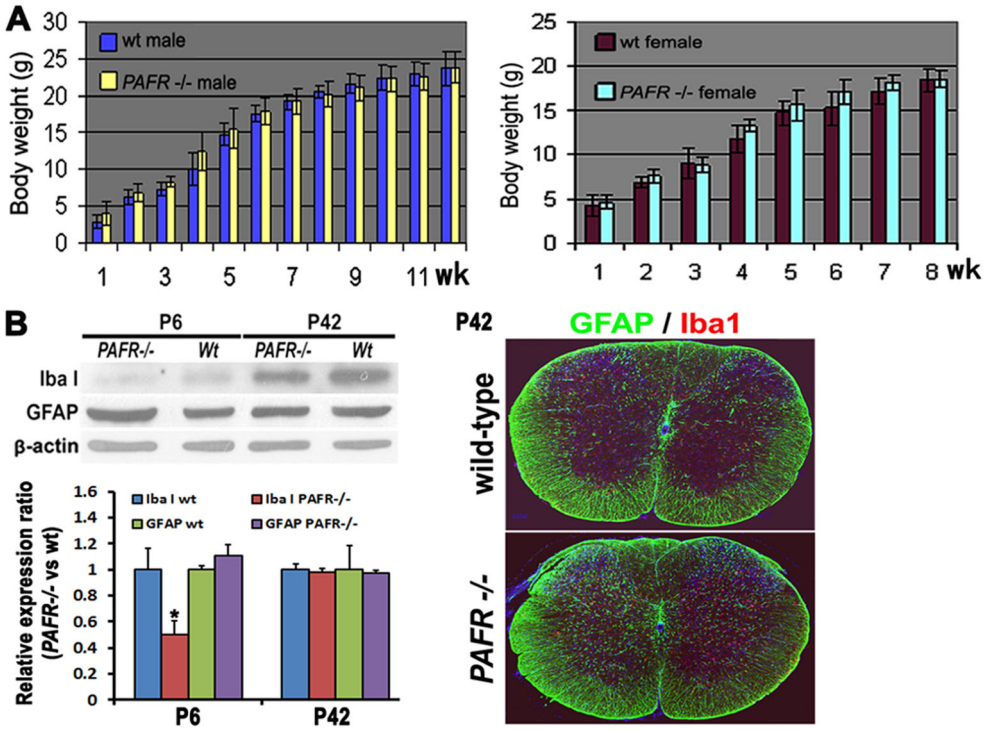

Fig. 1 Development of gross growth and glial cells in *PAFR* null mutant mice. **a** Body weights in male (n=8) and female (n=8) wild-type and *PAFR* null mutant mice, respectively (p>0.05). **b** Iba1^{+} resting/surveying microglia and GFAP^{+} astrocytes in wild-type and *PAFR* null mutant spinal cords. *Scale bar* at 100 μm. Expression of Iba1 but not GFAP in *PAFR* null mutant spinal cords was significantly lower than that in wild-type ones at P6. However, their expressions did not show any difference between wild-type and *PAFR* null mutant spinal cords at P42. *Asterisk* represents p<0.05 (n=3)

the entire dorsal columns and partial corticospinal tracts, and evaluated the functional recovery by measuring forelimb strength and rotarod performance following cervical SCI. The baseline performance of either grip or rotarod test was similar in both *PAFR* null mutant and wild-type sham mice. After the SCI, *PAFR−/−* mice regained more forelimb strength after just 3 dpi (Fig. 3a) and showed better rotarod performance after 7 dpi (Fig. 3b) compared to wild-type injured mice. After 6 weeks, forelimb strength and rotarod running capability recovered (65.58±12.86 and 48.94±8.94 %) in *PAFR−/−* mice, compared to those (29.56±11.02 and 27.35±9.65 %) in wild-type mice, respectively.

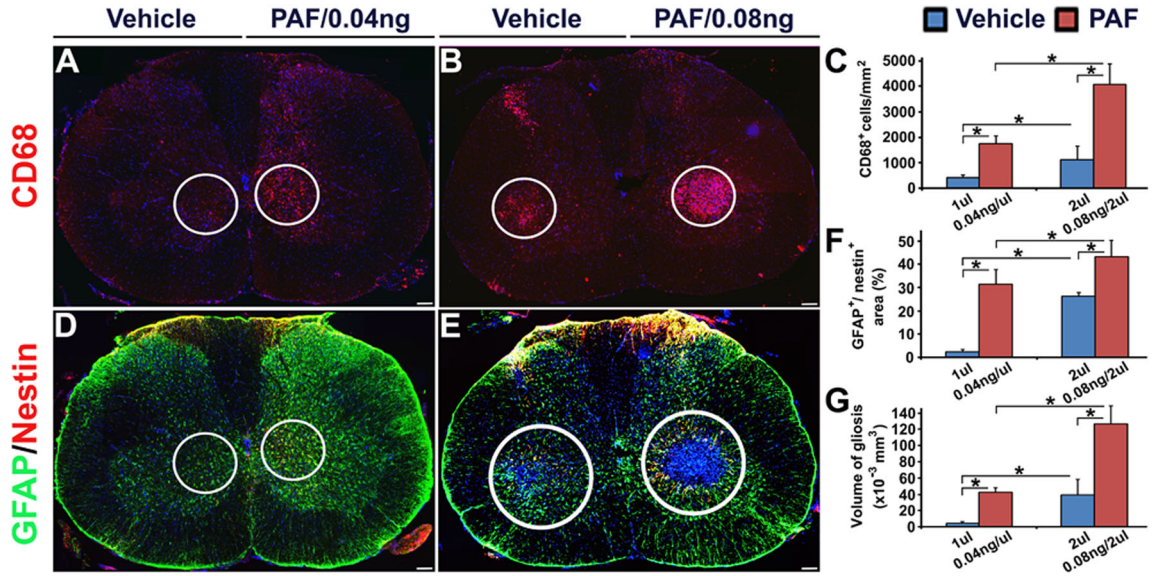

Fig. 2 Intraspinal injection of a low-dose (**a**, **d**) or high-dose (**b**, **e**) PAF (*right side*) and DMSO vehicle solution (*left side*) in 8-week-old wild-type mice. Activated microglia (**a**–**c**) or astrocytes (**d**–**f**) were labeled by anti-CD68 antibody (**a** and **b**) or anti-GFAP and anti-nestin antibodies (**d** and **e**), and the volume of gliosis was quantitatively analyzed (**g**). *Scale bar* at 100 μm. *Asterisk* represents p<0.05. Only a few CD68^{+} microglia and GFAP^{+}/nestin^{+} astrocytes were found in the unilateral side with vehicle injection. In contrast, many more microglia and astrocytes were activated and confined in the area surrounding the site of injection with PAF via a dose-dependent manner, resulting in a larger lesion volume

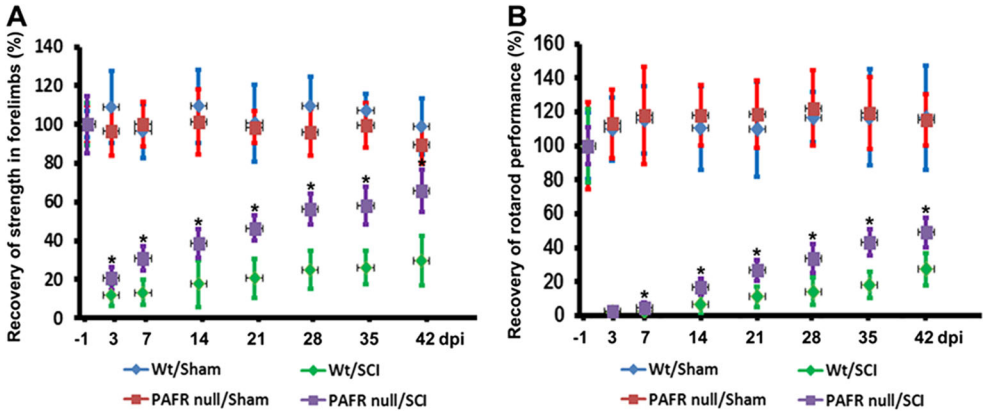

Fig. 3 Forelimb strength (**a**) and rotarod performance (**b**) in 6- to 8-week-old wild-type and *PAFR* null mutant mice with or without cervical SCI. Wild-type sham mice (n=8), *PAFR*−/− sham mice (n=5), Wild-type SCI mice (n=10), and *PAFR*−/− SCI mice (n=8). *Asterisk* represents $p<0.05$ (*PAFR* null/SCI vs. Wt/SCI). Compared to wild-type injured mice, significant functional improvement of forelimb strength and rotarod performance was observed in *PAFR*−/− SCI mice

Microglia Activation and Inflammatory Response in *PAFR* Null Mutant and Wild-Type Mice After Cervical SCI

Microglia are considered "tissue macrophages" in the CNS, owing to their phenotype and reactivity following any disturbance or loss of homeostasis that indicates real or potential danger to the CNS. In reactive gliosis of SCI, microglia can be activated around the lesion area and regulate the inflammatory process by releasing cytokines. Cluster of differentiation 68 (CD68) is expressed in monocytes/macrophages and activated microglia. In the injured spinal cords, an abundance of $CD68^+$ macrophages/activated microglia were aggregated in the epicenter of the lesion and its adjacent area at 3 dpi (Fig. 4d, j). The accumulation of $CD68^+$ cells reached a peak around 7 dpi and declined thereafter (Fig. 4e, f, k–m). Surprisingly, many more $CD68^+$ cells were observed in the epicenter in *PAFR*−/− mice at 3 and 7 dpi (Fig. 4d–f, j–m). Meanwhile, expression of pro-inflammatory cytokine IL-6 was boosted after the SCI in null mutants but not significantly as occurred in wild-type mice at 7 dpi. Five weeks later, expression of IL-6 in *PAFR* −/− injured spinal cords returned to the sham level; however, its expression in wild-type injured spinal cords was still higher than that in sham ones (Fig. 4n).

Activation of Astrocytes and ECM Remodeling in *PAFR* Null Mutant SCI Mice

Astrocytes are the most abundant cells in the CNS. Activated by microglia, astrocytes make contributions to reactive gliosis by overexpressing intermediate filament proteins, in particular GFAP, nestin, and vimentin, and other molecules (e.g., CSPGs, tenascins, and collagen), which play the major role in scar formation after SCI. As described in previous reports, expressions of GFAP and vimentin were dramatically elevated in injured wild-type spinal segments (Fig. 5o, p). Activated astrocytes co-labeled with GFAP and nestin were localized in the region surrounding the epicenter, especially in white matter (Fig. 5g, i, k). In contrast, although expressions of GFAP, vimentin, and nestin were also increased in *PAFR* null mutant spinal cords after the SCI, they were significantly inhibited and downregulated at the later phase (Fig. 5h, j, l, m, o, p). More interestingly, nestin was almost extinguished in activated $GFAP^+$ astrocytes of *PAFR* null mutant SCI mice in white matter (Fig. 5h, j, l, arrows). Compared to *PAFR* null mutant mice, wild-type mice produced larger lesion core volumes after the SCI (N).

Reactive astrocytes contribute significantly to the release of the inhibitory ECM components after CNS injury [31]. After the CNS injury, over-reactive astrocytes at the lesion site form the GS and alter the composition of ECM dramatically. ECM components including CSPGs and tenascins are markedly upregulated in astrocytes [32, 33]. Compared to the sham cords, inhibitory proteoglycan CS56 was highly expressed in injured wild-type and *PAFR* null mutant spinal cords starting at 3 dpi but much less in injured *PAFR* null mutants than that in wild-type mice (Fig. 6a b). Supporting this observation, neurocan (CSPG3), considered as a neurite growth inhibitor, was inhibited in *PAFR*−/− SCI mice (Fig. 6c).

Enhanced Axonal Plasticity and/or Regeneration *PAFR* Null Mutant Mice After Cervical SCI

Inhibiting the astroglial activation and/or remodeling the ECM of astrocytic scar enhances axonal plasticity and regeneration and promotes functional improvement in rodent SCI models [34–37]. Attenuated reactive gliosis and lower level of inhibitory ECM molecules in *PAFR* null mutant SCI mice suggest that blocking PAF signaling may promote axonal plasticity and/or regeneration after injury. To assess the axonal plasticity and/or regeneration, we conducted double immunostaining and Western blot with anti-NF200 and anti-phospho-

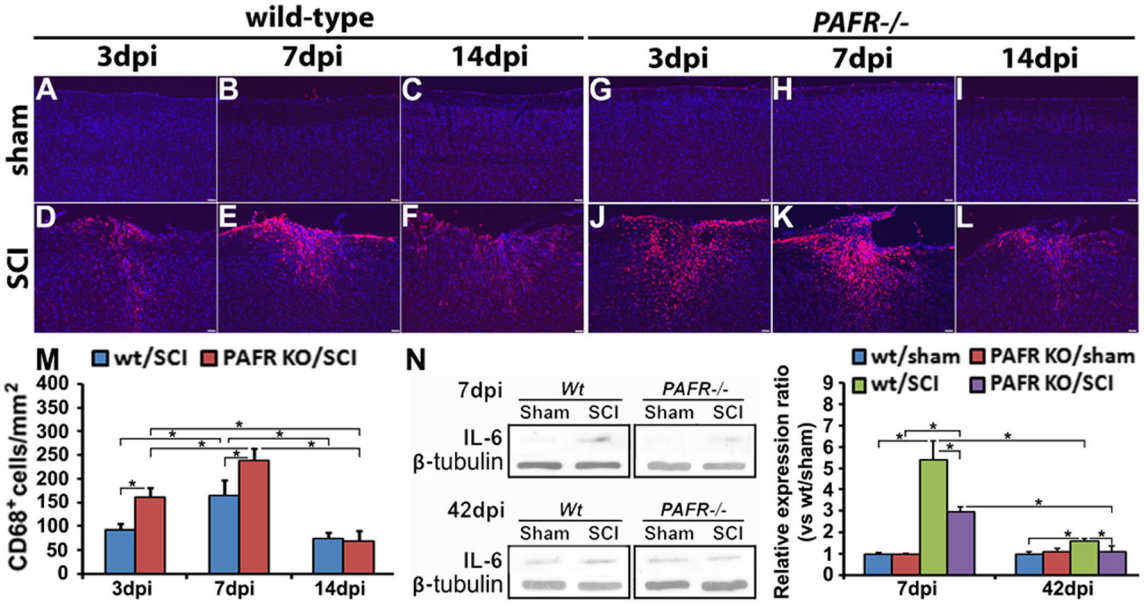

Fig. 4 Inflammatory response in sham (**a**–**c**, **g**–**i**) and cervical injured (**d**–**f**, **j**–**l**) spinal cords of wild-type (**a**–**f**) and *PAFR* null mutant (**g**–**l**) mice. **a**–**m** Activation of microglia ($CD68^+$) in epicenter of injured wild-type and *PAFR* null mutant spinal cords. *Scale bar* at 100 μm. *Asterisk* represents $p<0.05$. $CD68^+$ cells reached a peak around 7 dpi and declined thereafter. More $CD68^+$ cells were found surrounding the epicenter of lesion in *PAFR*−/− mice than those in wild-type mice during the acute phase after SCI. (N) Lower expression of pro-inflammatory cytokine IL-6 in injured spinal cords of *PAFR* null mutants compared to wild-type mice at 7 and 42 dpi. *Asterisk* represents $p<0.05$

NF200 antibodies. It has been reported that myelination is required for the phosphorylation of NF-H [38], and unmyelinated segments only have dephosphorylated NF-H [39, 40]. Consistent with these previous observations, myelinated axons labeled with anti-phospho-NF200 (red) alone or with anti-NF200 (yellow) were localized in the spinal white matter, and unmyelinated ones recognized by anti-NF200 (green) alone or with anti-phospho-NF200 (yellow) were restricted in the gray matter in both wild-type and *PAFR*−/− sham mice (Fig. 7a, e). At 3 dpi, more unmyelinated axons were found in the adjacent white matter area next to the lesion epicenter, indicating that the demyelinating process occurred after SCI (Fig. 7b, f). Four days later, most of the unmyelinated axons (arrowheads) and few myelinated fibers (arrows) existed in the region far away from the epicenter in wild-type SCI mice; however, unmyelinated axons and more myelinated fibers were still observed in the area next to the lesion in *PAFR*−/− mutants (Fig. 7c, g). Four weeks following cervical dorsal funiculotomy, more unmyelinated (arrowheads) and myelinated (arrows) fibers emerged again in the area next to the lesion border in *PAFR*−/− mutants compared to those in wild-type mice (Fig. 7d, h).

Systemic Administration of PAFR Antagonist to Promote Functional Recovery After Cervical SCI

Ginkgolide B (GB) is a natural-originated, highly selective, and competitive PAFR antagonist, which is regarded as having neuroprotective effects due to inhibition of inflammatory responses in the CNS [41]. Previous studies indicated that the acute phase of inflammation occurs during the first week after SCI in mice. Pro-inflammatory cytokines are released between 6 and 12 h after injury and peak at 4 dpi. However, the formation of GS starts around 14 dpi and continues during the subacute and chronic phases. To assess the effects of GB on the inflammatory responses and GS forming process, GB was administrated during the early acute phase (0–10 dpi) or the following the subacute to chronic phase (10–42 dpi). Indeed, systemic administration of GB for 42 days did not result in a change of forelimb grip strength nor rotarod performance in wild-type mice (Fig. 8a, b). Compared to the wild-type SCI mice with vehicle injections, mice with GB treatment for the first 10 days significantly regained their forelimb strength after 14 dpi, reached the peak at 28 dpi, and returned to the vehicle level after 35 dpi. Similarly, mice with GB treatment between 10 and 42 dpi also significantly improved their forelimb strength after 14 dpi and continued the strength recovery until 42 dpi (Fig. 8c). For the rotarod assessment, only mice with late-stage treatment showed an impressive performance after 28 dpi (Fig. 8d). Six weeks after the injury, GB treatment during the subacute and chronic phases had better therapeutic effect on functional recovery (grip 66.3±11.8 %; rotarod 61.7±12.9 %) than that during the acute phase (grip 50.9±7.7 %; rotarod 45±14.1 %) in the cervical SCI mice. Notably, the wild-type SCI mice administrated with 1× PBS containing 50 % DMSO showed a greater improvement in grip (49.3±18.4 vs. 29.56±11.02 %,

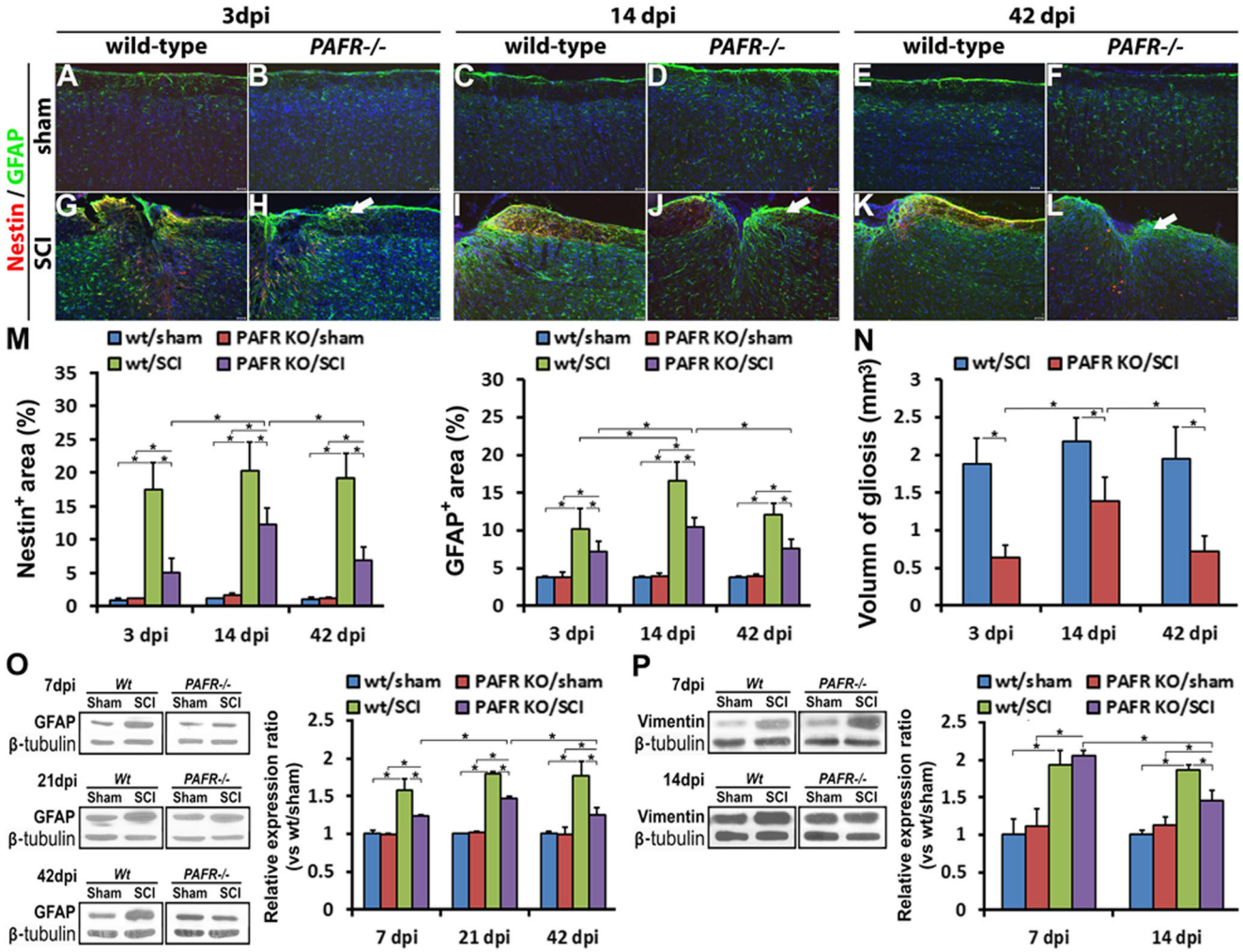

Fig. 5 Reactive astrocytes in sham (**a**–**f**) and cervical injured (**g**–**l**) spinal cords of wild-type (**a**, **g**, **c**, **i**, **e**, **k**) and *PAFR* null mutant (**b**, **h**, **d**, **j**, **f**, **l**) mice at 3, 14, and 42 dpi. *Scale bar* at 100 μm. More nestin^{+}/GFAP^{+} astrocytes were localized in the surrounding region of epicenter (especially for white matter area) after SCI in the wild-type mice, compared to those in *PAFR* null mutant mice (**g**–**l**). Expressions of nestin (**m**), GFAP (**m**, **o**), and vimentin (**p**) were increased in *PAFR* null mutant spinal cords after SCI but dramatically inhibited and downregulated at the later phase. Quantitative analysis revealed significantly larger lesion core volumes in wild-type injured spinal cords (N). *Asterisks* represent $p<0.05$

$p<0.01$) and rotarod performance (46.4±12.5 vs. 27.35 ±9.65 %, $p<0.01$) than wild-type injured mice, probably due to the anti-inflammatory, anti-oxidative, and analgesic properties of DMSO [42].

Discussion

For several decades, GS that occurs during the chronic stage of secondary lesion after SCI has been considered one of the major obstacles for axonal regeneration. As two major cellular components of reactive gliosis, growing evidences indicate a tightly reciprocal modulation between microglia and astrocytes during the GS formation [43]. Under the pathological conditions in the CNS, microglia are activated earlier than astrocytes. The cytokines released from activated microglia and other cells, such as macrophages and infiltrating immune T cells, may function as either initial molecular inducers (e.g., IL-6, IFNγ) or repressors (e.g., IL-10) of GS formation during the acute phase of SCI. On the other hand, reactive astrocytes may secrete some molecules to maintain microglia presenting in the lesion site and persistent inflammatory response during the chronic phase of CNS injury. Thus, modulation combining both the inflammatory response and GS will create a more nourishing niche for axonal regeneration. Here, we reported that blocking PAF signaling attenuated reactive gliosis and to some extent promoted axonal plasticity/regeneration and functional recovery, suggesting that PAF likely participates in modulating both inflammatory response and GS formation after the SCI.

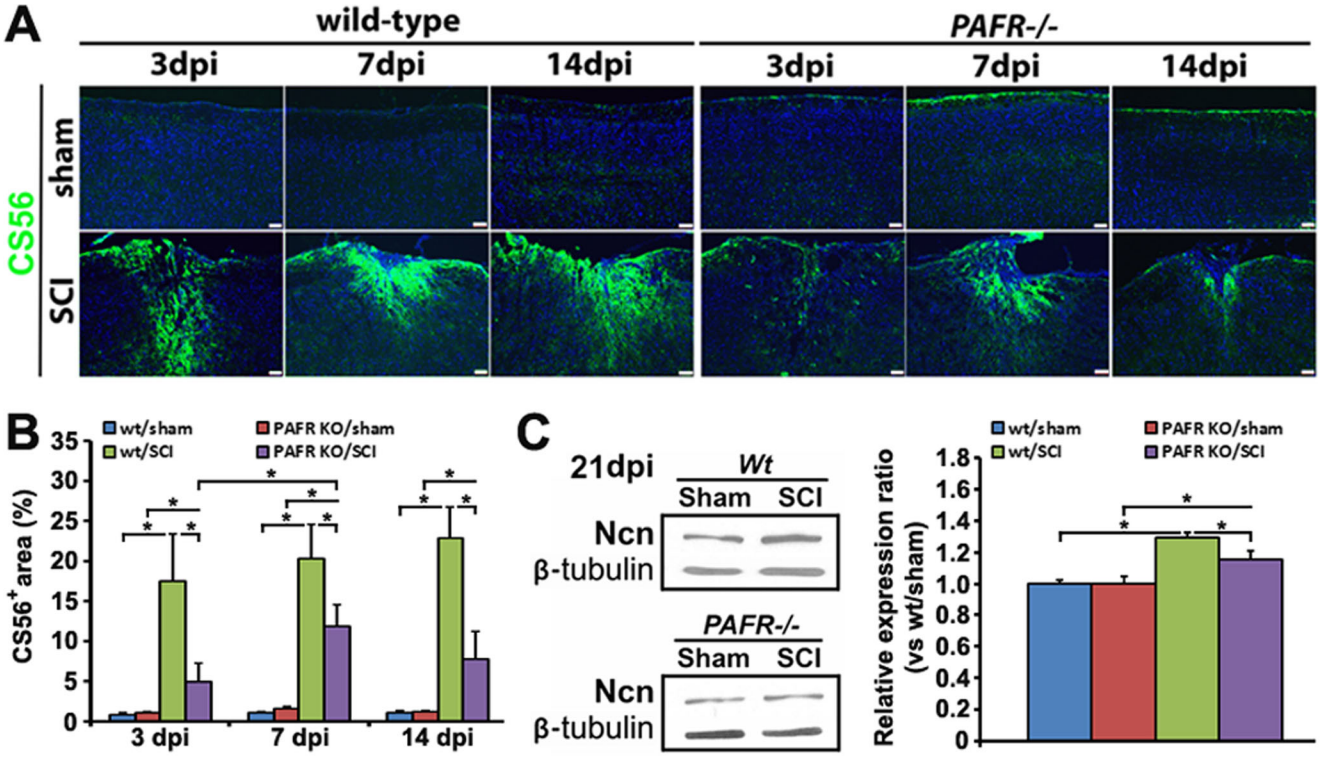

Fig. 6 Expression of inhibitory proteoglycan CS56 (**a**, **b**) and neurocan (**c**) in epicenter of injured wild-type and *PAFR* null mutant spinal cords. *Scale bar* at 100 μm. *Asterisk* represents $p<0.05$. Inhibitory proteoglycan CS56 and neurocan were highly expressed in injured wild-type and *PAFR* null mutant spinal cords but much less in injured *PAFR* null mutants than that in wild-type mice

PAF-Induced Inflammation, Demyelination, and Axonal Dieback/Retraction After the SCI

Accumulating evidence suggests that inflammation seems to be a critical step in secondary degeneration after SCI and causal to GS formation. It was well-known that PAF signaling is responsible for pro-inflammatory responses, which is involved in pathological consequences by eliciting inflammation and cytotoxicity [44]. Phospholipases A_2 (PLA_2), a diverse family of lipolytic enzymes, plays a key role in

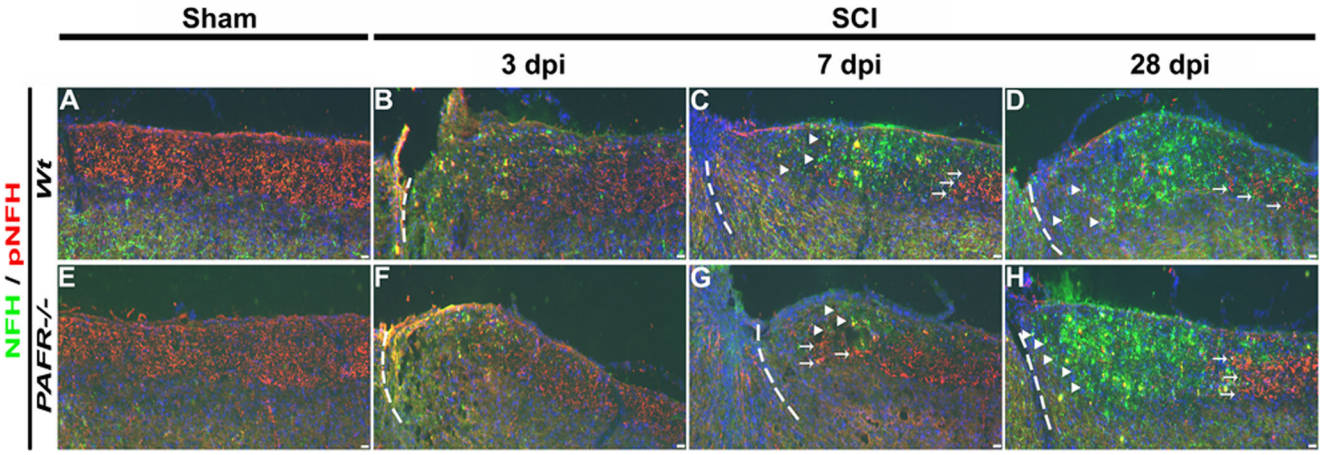

Fig. 7 Myelinated axon labeled by anti-NFH and anti-phosphorylated NFH antibodies in sham (**a**, **e**) and cervical injured (**b**–**d**, **f**–**h**) spinal cords of wild-type (**a**–**d**) and *PAFR* null mutant (**e**–**h**) mice. *Arrows* indicate myelinated fibers (*red or yellow*). *Arrowheads* indicate demyelinated fibers (*green*). *Scale bar* at 100 μm. At 3 dpi, more unmyelinated axons were found in the *adjacent white matter area* next to the lesion epicenter, indicating that the demyelinating process occurred after SCI. Four days later, most of unmyelinated axons (*arrowheads*) and few myelinated fibers (*arrows*) existed in the region far away from the epicenter in wild-type SCI mice; however, unmyelinated axons and more myelinated fibers were still observed in the area next to the lesion in *PAFR*−/− mutants. Four weeks after the SCI, more unmyelinated (*arrowheads*) and myelinated (*arrows*) fibers emerged again in the area next to the lesion border in *PAFR*−/− mutants compared to those in wild-type mice

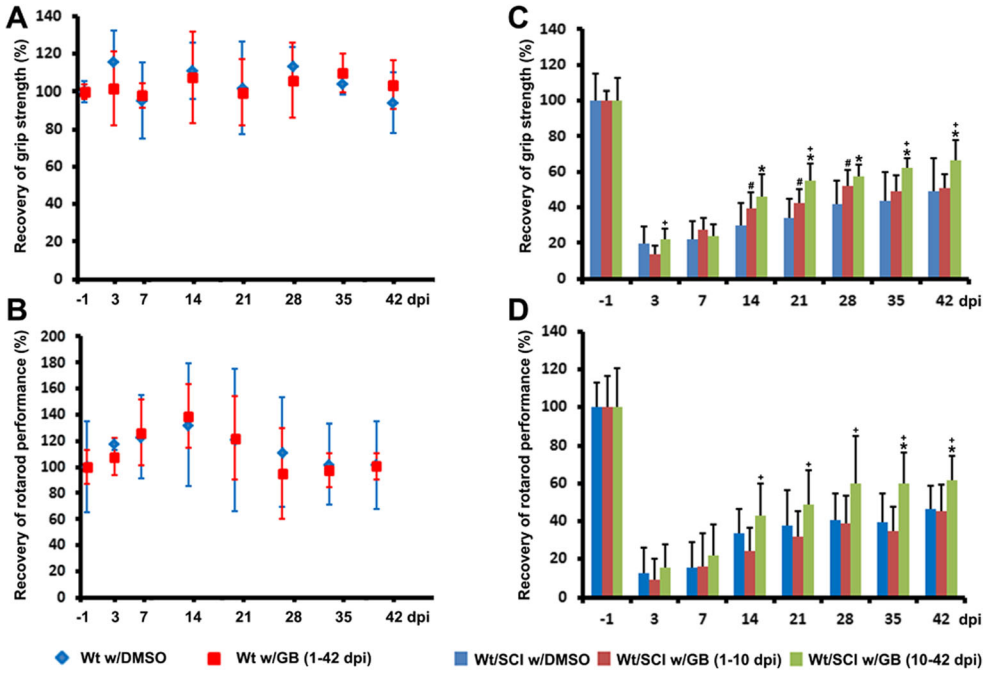

Fig. 8 Functional recovery of forelimb strength (**a**, **c**) and rotarod performance (**b**, **d**) in 8-week-old wild-type (**a**, **b**) and wild-type with SCI (**c**, **d**) mice treated with DMSO vehicle solution or GB. *Asterisk* represents $p<0.05$, SCI w/GB(10-42dpi) vs. SCI w/DMSO. *Number sign* represents $p<0.05$, SCI w/GB(1-10dpi) vs. SCI w/DMSO. *Plus sign* represents $p<0.05$, GB(10-42dpi) vs. SCI w/GB (1–10 dpi). The wild-type mice injected with GB for 42 days ($n=4$) demonstrated similar forelimb strength and rotarod performance as those wild-type mice injected with DMSO vehicle solution ($n=4$). Compared to the wild-type SCI mice injected with DMSO vehicle solution for 42 days after injury ($n=10$), administration of GB during the subacute and chronic phases ($n=7$) showed an enhanced functional recovery than that during the acute inflammatory phase ($n=12$) after SCI

mediating mammalian CNS injury. As its major intracellular form, $cPLA_2$ presenting in both the brain [45, 46] and spinal cord [47] hydrolyzes membrane phospholipids at the sn-2 position to lease free fatty acids (arachidonic acid or docosahexaenoic acid) and produce lysophospholipids [21, 48, 49], including lyso-PAF, the precursor of PAF. Following SCI in rodents, activity and expression of $cPLA_2$ are significantly increased. Activated $cPLA_2$ is localized mainly in neurons, oligodendrocytes, and microglia but not astrocytes [20, 50], suggesting that a high level of PAF is likely synthesized in neurons, oligodendrocytes, and microglia. It has been reported that tissue levels of PAF are elevated by approximately 13- to 20-fold in the injured spinal cord compared with that in the normal spinal cord [19, 22]. In the present study, exogenous PAF induced activation of microglia ($CD68^+$ cells) within the epicenter of injection and adjacent area in normal wild-type spinal cords (Fig. 2a–c). Similarly, microglia were dramatically activated surrounding the laceration lesion after SCI (Fig. 4a–f, m).

In the *PAFR−/−* mutant CNS, the effect of PAF signaling is assumed to be blocked due to the deletion of its receptor from those target cells including neurons, microglia, astrocytes, and oligodendrocyte precursor cells. Surprisingly, activation of microglia ($CD68^+$ cells) was significantly enhanced but not suppressed in *PAFR−/−* mutant mice with dorsal laceration SCI between 3 and 14 dpi (Fig. 4g–m), indicating that a PAFR-independent modulation [51–53] and a PAFR-dependent feedback inhibition on microglia may exist. A previous report showed that the microglia, astrocytes, infiltrating immune T cells, and macrophages synthesize and release pro-inflammatory cytokines 6–12 h after injury with a peak at 4 days [54]. Consistently, lower expression of pro-inflammatory cytokine IL-6 in *PAFR−/−* mutant mice after the SCI suggests an attenuated inflammatory response compared to what occurs in wild-type mice (Fig. 4n). Taken together, our findings indicate that PAF signaling contributes to microglial activation and inflammatory response via receptor-independent and/or receptor-dependent mechanisms after the SCI. Previous studies indicated that PAFR expression is restricted to apoptotic neurons and microglia but is rarely detected in surviving neurons [55], and genetic depletion of PAFR significantly prevents neuronal degeneration [56]. Supporting these observations, myelin breakdown and axonal dieback in knockout mice occurred later than those in wild-type mice at the same time points during the acute phase after the injury (Fig. 7b, c, f, g), suggesting that neuroprotection when PAF signaling was blocked by disruption of its receptor.

PAF-Activated Reactive Astrocytes and ECM Remodeling After the SCI

Reactive astrocytes are the main cellular component of the GS, which is characterized by the cellular hypertrophy and an abnormal increase in the number. After the injury, astrocytes are likely to react promptly to the damage, which undergo morphological changes, extend their processes, and increase synthesis of intermediate filament proteins. Upregulation of intermediate filament proteins, in particular GFAP, vimentin, and nestin in astrocytes, is regarded as the hallmark of reactive astrocytes. As a major intermediate filament protein in mature astrocytes, significantly increased expression of GFAP and GFAP$^+$ reactive astrocytes gathered from the area surrounding the epicenter was observed after the PAF injection in wild-type mice (Fig. 2d–f) or SCI in both wild-type and PAFR null mutant mice (Fig. 5a–l). It has been reported that reexpression of vimentin in reactive astrocytes following the injury is indicative of these cells recapitulating developmental migratory processes [57]. We found that the expression level of vimentin was elevated in injured spinal tissues as well (Fig. 5p). Nevertheless, expressions of nestin, GFAP, and vimentin in *PAFR−/−* knockout mice were much less than those in wild-type mice, especially at the late chronic SCI phase (Fig. 5m, o, p). Nestin-immunopositive cells can be seen in reactive astrocytes in response to the CNS injury [58]. Of note, nestin$^+$ astrocytes were almost extinguished in the spinal white matter of *PAFR−/−* mutant mice where the boosted expression was found in wild-type mice (Fig. 5h, j, l, arrows). Since PAFR is highly expressed in astrocytes [12], these findings suggest that PAF may activate astrocytes via its receptor. Recent in vivo studies identified two cellular origins of astrocytes in the GS after the SCI, preexisting GFAP-positive astrocytes and ependymal cell-derived GFAP-negative astrocytes [59, 60], indicating heterogeneous cellular components of reactive astrocytes in the GS. Nestin-negative astrocytes in spinal white matter may provide a clue to further identify the different origin and subpopulation of reactive astrocytes.

On the other hand, reactive astrocytes contribute significantly to the release of inhibitory ECM components after the CNS injury [31], which form a dense GS around the injured lesion to pose physical/chemical barriers and suppress axon regrowth [61, 62]. In *PAFR−/−* mutants, expressions of inhibitory proteoglycan CS56 and neurocan were significantly inhibited after the injury (Fig. 6). In accordance with the reduction of glial scar formation (Fig. 5n), more unmyelinated (arrowheads) and myelinated (arrows) emerged in the adjacent area next to the lesion border in *PAFR−/−* mutants compared to that in wild-type mice (Fig. 7d, h) at 3 weeks following cervical dorsal funiculotomy. Taken together, all these findings indicate that disruption of PAF signaling via genetic ablation of its receptor can inhibit the activation of astrocytes, remodel the ECM components, and promote axonal plasticity and/or regrowth.

The underlying mechanisms leading to astrogliosis are not yet completely understood. Growing evidence suggests that activated macrophages/microglia may contribute to the subsequent activation of astrocytes following CNS injury, and astroglial activation is triggered by a number of cytokines, chemokines, growth factors, and transcription factors [63]. As the most important pro-inflammatory cytokines secreted by macrophages/microglia, IL-1, IL-2, IL-6, and TNF-α, play important roles to activate the astrocytes via their receptors in the acute phase of CNS injury [64–67]. For example, excessive expression of IL-6 in mice showed marked gliosis and neurological signs even after mild injury of the spinal cord [68]. In IL-6 knockout mice, reactive GFAP-positive astrocytes and gliosis are drastically inhibited [69]. Blocking the IL-6 signal with IL-6 receptor antibody after a contusive injury in mice can repress the GS formation at the epicenter [65]. Thus, restrained inflammatory response caused by PAF receptor disruption may also repress the GS formation indirectly via limited synthesis of pro-inflammatory cytokines such as IL-6 (Fig. 4n). Recent study showed that the selective and competitive PAFR antagonist GB promotes the recovery of sensorimotor function at the acute phase in SCI rats and significantly suppresses the JAK/STAT signals boosted during the first 3 days after injury [70], suggesting that GB may inhibit the proinflammatory activation of microglia [71]. In our study, administration of GB not only enhances functional recovery during the acute inflammatory phase (0–10 dpi) but also more significantly improves the sensorimotor function during the subacute and chronic phases (10–42 dpi) after SCI as well (Fig. 8). However, direct evidence and intracellular mechanisms on PAFR-mediated astrogliosis could be revealed when PAFR conditional knockout mice are available.

Combinational Therapy of Anti-inflammation, ECM Remodeling, and GS Modification After the SCI

The current treatment for SCI clinically focuses on anti-inflammation and neuroprotection during the acute and subacute phases. GS modification therapy is still under exploration. Cumulative evidence indicates that reactive astrocytes and their products may contribute to induce a secondary peak of macrophages/microglia presenting in the lesion site and maintain a persistent inflammatory response during the chronic phase of the CNS injury. Reactive astrocytes also secrete the same inflammatory cytokines that may in turn activate microglia and cause the secondary injury [72]. Either microglia or astrocytes can release a battery of signal molecules to feedback themselves to serve cross-talk with adjacent CNS cells, i.e., neurons, oligodendrocytes, astrocytes, microglia, and infiltrating immune cells. Thus, identification of a target regulating both processes of early inflammation and late GS

formation may offer a novel combinatorial therapy after the SCI. The PAFR antagonists have been applied in clinical trials of immunomodulatory therapy, anti-inflammation, and treatment of neurodegenerative diseases. In this study, we demonstrated that genetic ablation of PAFR or systemic administration of PAFR antagonist GB promotes functional recovery after SCI probably not only via anti-inflammatory/neuroprotective effects but also via modification of astrogliosis (Figs. 3 and 8), which provides fundamental evidence for potential application of PAFR antagonists in SCI treatment.

Acknowledgments This work was supported by pilot grants of NIH (P30 GM103507-04) and Department of Pediatrics, NSFC (81400998), NSFC (81360195), State Key Program of NSFC (81330042), Sino-Russian Joint Research Program of MSTC (2014DFR31210), Key Program of Tianjin STCC (13RCGFSY19000, 14ZCZDSY00044), and CSC scholarship. The authors would like to thank Dr. Theo Hagg for his critical comments on experimental design.

Conflict of Interest The authors report no conflicts of interest.

References

1. Preston E, Webster J, Small D (2001) Characteristics of sustained blood-brain barrier opening and tissue injury in a model for focal trauma in the rat. J Neurotrauma 18(1):83–92
2. Bush TG, Puvanachandra N, Horner CH, Polito A, Ostenfeld T, Svendsen CN, Mucke L, Johnson MH et al (1999) Leukocyte infiltration, neuronal degeneration, and neurite outgrowth after ablation of scar-forming, reactive astrocytes in adult transgenic mice. Neuron 23(2):297–308
3. Faulkner JR, Herrmann JE, Woo MJ, Tansey KE, Doan NB, Sofroniew MV (2004) Reactive astrocytes protect tissue and preserve function after spinal cord injury. J Neurosci : Off J Soc Neurosci 24(9):2143–2155
4. Fitch MT, Silver J (2008) CNS injury, glial scars, and inflammation: inhibitory extracellular matrices and regeneration failure. Exp Neurol 209(2):294–301
5. Su Z, Yuan Y, Chen J, Zhu Y, Qiu Y, Zhu F, Huang A, He C (2011) Reactive astrocytes inhibit the survival and differentiation of oligodendrocyte precursor cells by secreted TNF-α. J Neurotrauma 28(6):1089–1100
6. Wang XF, Huang LD, Yu PP, Hu JG, Yin L, Wang L, Xu XM, Lu PH (2006) Upregulation of type I interleukin-1 receptor after traumatic spinal cord injury in adult rats. Acta Neuropathol 111(3):220–228
7. Ishii S, Shimizu T (2000) Platelet-activating factor (PAF) receptor and genetically engineered PAF receptor mutant mice. Prog Lipid Res 39(1):41–82
8. Yue TL, Feuerstein GZ (1994) Platelet-activating factor: a putative neuromodulator and mediator in the pathophysiology of brain injury. Crit Rev Neurobiol 8(1–2):11–24
9. Kumar R, Harvey SA, Kester M, Hanahan DJ, Olson MS (1988) Production and effects of platelet-activating factor in the rat brain. Biochim Biophys Acta 963(2):375–383
10. Sogos V, Bussolino F, Pilia E, Torelli S, Gremo F (1990) Acetylcholine-induced production of platelet-activating factor by human fetal brain cells in culture. J Neurosci Res 27(4):706–711
11. Bito H, Nakamura M, Honda Z, Izumi T, Iwatsubo T, Seyama Y, Ogura A, Kudo Y et al (1992) Platelet-activating factor (PAF) receptor in rat brain: PAF mobilizes intracellular Ca2+ in hippocampal neurons. Neuron 9(2):285–294
12. Brodie C (1994) Functional PAF receptors in glia cells: binding parameters and regulation of expression. Int J Dev Neurosci : Off J Int Soc Dev Neurosci 12(7):631–640
13. Hostettler ME, Knapp PE, Carlson SL (2002) Platelet-activating factor induces cell death in cultured astrocytes and oligodendrocytes: involvement of caspase-3. Glia 38(3):228–239
14. Mori M, Aihara M, Kume K, Hamanoue M, Kohsaka S, Shimizu T (1996) Predominant expression of platelet-activating factor receptor in the rat brain microglia. J Neurosci : Off J Soc Neurosci 16(11):3590–3600
15. Bozlu G, Atici A, Turhan AH, Polat A, Nayci A, Okuyaz C, Taskinlar H (2007) Platelet-activating factor antagonist (ABT-491) decreases neuronal apoptosis in neonatal rat model of hypoxic ischemic brain injury. Brain Res 1143:193–198
16. Row BW, Kheirandish L, Li RC, Guo SZ, Brittian KR, Hardy M, Bazan NG, Gozal D (2004) Platelet-activating factor receptor-deficient mice are protected from experimental sleep apnea-induced learning deficits. J Neurochem 89(1):189–196
17. Brochet B, Guinot P, Orgogozo JM, Confavreux C, Rumbach L, Lavergne V (1995) Double blind placebo controlled multicentre study of ginkgolide B in treatment of acute exacerbations of multiple sclerosis. The Ginkgolide Study Group in multiple sclerosis. J Neurol Neurosurg Psychiatry 58(3):360–362
18. Hostettler ME, Carlson SL (2002) PAF antagonist treatment reduces pro-inflammatory cytokine mRNA after spinal cord injury. Neuroreport 13(1):21–24
19. Lindsberg PJ, Jacobs TP, Paakkari IA, Hallenbeck JM, Feuerstein G (1990) Effect of systemic platelet-activating factor (PAF) on the rabbit spinal cord microcirculation. J Lipid Mediat 2(1):41–58
20. Liu NK, Zhang YP, Titsworth WL, Jiang X, Han S, Lu PH, Shields CB, Xu XM (2006) A novel role of phospholipase A2 in mediating spinal cord secondary injury. Ann Neurol 59(4):606–619
21. Liu NK, Xu XM (2010) Phospholipase A2 and its molecular mechanism after spinal cord injury. Mol Neurobiol 41(2–3):197–205
22. Zhang J, Wang Z, Lin A, Li S, Wen F, Yao H (2011) Effect of buying huanwu decoction on the content of platelet activating factor in spinal cord tissue of rats with spinal cord injury. Chin J Inf TCM 18(11):46–48
23. Ishii S, Kuwaki T, Nagase T, Maki K, Tashiro F, Sunaga S, Cao WH, Kume K et al (1998) Impaired anaphylactic responses with intact sensitivity to endotoxin in mice lacking a platelet-activating factor receptor. J Exp Med 187(11):1779–1788
24. Zhang YP, Iannotti C, Shields LB, Han Y, Burke DA, Xu XM, Shields CB (2004) Dural closure, cord approximation, and clot removal: enhancement of tissue sparing in a novel laceration spinal cord injury model. J Neurosurg 100(4 Suppl Spine):343–352
25. Yu P, Zhang YP, Shields LB, Zheng Y, Hu X, Hill R, Howard R, Gu Z et al (2011) Inhibitor of DNA binding 2 promotes sensory axonal growth after SCI. Exp Neurol 231(1):38–44
26. Gow A, Southwood CM, Li JS, Pariali M, Riordan GP, Brodie SE, Danias J, Bronstein JM et al (1999) CNS myelin and sertoli cell tight junction strands are absent in Osp/claudin-11 null mice. Cell 99(6):649–659
27. Shiotsuki H, Yoshimi K, Shimo Y, Funayama M, Takamatsu Y, Ikeda K, Takahashi R, Kitazawa S et al (2010) A rotarod test for evaluation of motor skill learning. J Neurosci Methods 189(2):180–185
28. Cai J, Qi Y, Hu X, Tan M, Liu Z, Zhang J, Li Q, Sander M et al (2005) Generation of oligodendrocyte precursor cells from mouse dorsal spinal cord independent of Nkx6 regulation and Shh signaling. Neuron 45(1):41–53
29. Cai J, Zhu Q, Zheng K, Li H, Qi Y, Cao Q, Qiu M (2010) Co-localization of Nkx6.2 and Nkx2.2 homeodomain proteins in differentiated myelinating oligodendrocytes. Glia 58(4):458–468

30. Cai J, Tuong CM, Zhang Y, Shields CB, Guo G, Fu H, Gozal D (2012) Mouse intermittent hypoxia mimicking apnoea of prematurity: effects on myelinogenesis and axonal maturation. J Pathol 226(3):495–508
31. Stichel CC, Muller HW (1998) The CNS lesion scar: new vistas on an old regeneration barrier. Cell Tissue Res 294(1):1–9
32. Asher RA, Morgenstern DA, Fidler PS, Adcock KH, Oohira A, Braistead JE, Levine JM, Margolis RU et al (2000) Neurocan is upregulated in injured brain and in cytokine-treated astrocytes. J Neurosci 20(7):2427–2438
33. Gutowski NJ, Newcombe J, Cuzner ML (1999) Tenascin-R and C in multiple sclerosis lesions: relevance to extracellular matrix remodelling. Neuropathol Appl Neurobiol 25(3):207–214
34. Cafferty WBJ, Yang S-H, Duffy PJ, Li S, Strittmatter SM (2007) Functional axonal regeneration through astrocytic scar genetically modified to digest chondroitin sulfate proteoglycans. J Neurosci 27(9):2176–2185
35. Ito M, Natsume A, Takeuchi H, Shimato S, Ohno M, Wakabayashi T, Yoshida J (2009) Type I interferon inhibits astrocytic gliosis and promotes functional recovery after spinal cord injury by deactivation of the MEK/ERK pathway. J Neurotrauma 26(1):41–53
36. Jeong SR, Kwon MJ, Lee HG, Joe EH, Lee JH, Kim SS, Suh-Kim H, Kim BG (2012) Hepatocyte growth factor reduces astrocytic scar formation and promotes axonal growth beyond glial scars after spinal cord injury. Exp Neurol 233(1):312–322
37. Menet V, Prieto M, Privat A, Ribotta MGY (2003) Axonal plasticity and functional recovery after spinal cord injury in mice deficient in both glial fibrillary acidic protein and vimentin genes. Proc Natl Acad Sci 100(15):8999–9004
38. de Waegh SM, Lee VM, Brady ST (1992) Local modulation of neurofilament phosphorylation, axonal caliber, and slow axonal transport by myelinating Schwann cells. Cell 68(3):451–463
39. Hsieh ST, Kidd GJ, Crawford TO, Xu Z, Lin WM, Trapp BD, Cleveland DW, Griffin JW (1994) Regional modulation of neurofilament organization by myelination in normal axons. J Neurosci : Off J Soc Neurosci 14(11 Pt 1):6392–6401
40. Nixon RA, Paskevich PA, Sihag RK, Thayer CY (1994) Phosphorylation on carboxyl terminus domains of neurofilament proteins in retinal ganglion cell neurons in vivo: influences on regional neurofilament accumulation, interneurofilament spacing, and axon caliber. J Cell Biol 126(4):1031–1046
41. Maclennan KM, Darlington CL, Smith PF (2002) The CNS effects of Ginkgo biloba extracts and ginkgolide B. Prog Neurobiol 67(3): 235–257
42. Santos NC, Figueira-Coelho J, Martins-Silva J, Saldanha C (2003) Multidisciplinary utilization of dimethyl sulfoxide: pharmacological, cellular, and molecular aspects. Biochem Pharmacol 65(7): 1035–1041
43. Gao Z, Zhu Q, Zhang Y, Zhao Y, Cai L, Shields C, Cai J (2013) Reciprocal modulation between microglia and astrocyte in reactive gliosis following the CNS injury. Mol Neurobiol 48(3):690–701
44. Maclennan KM, Smith PF, Darlington CL (1996) Platelet-activating factor in the CNS. Prog Neurobiol 50(5–6):585–596
45. Kishimoto K, Matsumura K, Kataoka Y, Morii H, Watanabe Y (1999) Localization of cytosolic phospholipase A2 messenger RNA mainly in neurons in the rat brain. Neuroscience 92(3): 1061–1077
46. Molloy GY, Rattray M, Williams RJ (1998) Genes encoding multiple forms of phospholipase A2 are expressed in rat brain. Neurosci Lett 258(3):139–142
47. Ong WY, Horrocks LA, Farooqui AA (1999) Immunocytochemical localization of cPLA2 in rat and monkey spinal cord. J Mol Neurosci 12(2):123–130
48. Farooqui AA, Horrocks LA (2006) Phospholipase A_2-generated lipid mediators in the brain: the good, the bad, and the ugly. Neuroscientist 12(3):245–260
49. Leslie CC (1997) Properties and regulation of cytosolic phospholipase A2. J Biol Chem 272(27):16709–16712
50. Liu N-K, Deng L-X, Zhang YP, Lu Q-B, Wang X-F, Hu J-G, Oakes E, Bonventre JV et al (2014) Cytosolic phospholipase A2 protein as a novel therapeutic target for spinal cord injury. Ann Neurol 75(5): 644–658
51. O'Flaherty JT, Chabot MC, Redman J Jr, Jacobson D, Wykle RL (1989) Receptor-independent metabolism of platelet-activating factor by myelogenous cells. FEBS Lett 250(2):341–344
52. Ryan SD, Harris CS, Mo F, Lee H, Hou ST, Bazan NG, Haddad PS, Arnason JT et al (2007) Platelet activating factor-induced neuronal apoptosis is initiated independently of its G-protein coupled PAF receptor and is inhibited by the benzoate orsellinic acid. J Neurochem 103(1):88–97
53. Stoll LL, Denning GM, Kasner NA, Hunninghake GW (1994) Platelet-activating factor may stimulate both receptor-dependent and receptor-independent increases in [Ca2+] in human airway epithelial cells. J Biol Chem 269(6):4254–4259
54. Sobani ZA, Quadri SA, Enam SA (2010) Stem cells for spinal cord regeneration: current status. Surg Neurol Int 1:93
55. Bennett SAL, Chen J, Pappas BA, Roberts DCS, Tenniswood M (1998) Platelet activating factor receptor expression is associated with neuronal apoptosis in an in vivo model of excitotoxicity. Cell Death Differ 5(10):867–875
56. Kim BK, Shin EJ, Kim HC, Chung YH, Dang DK, Jung BD, Park DH, Wie MB et al (2013) Platelet-activating factor receptor knockout mice are protected from MPTP-induced dopaminergic degeneration. Neurochem Int 63(3):121–132
57. Wang K, Bekar LK, Furber K, Walz W (2004) Vimentin-expressing proximal reactive astrocytes correlate with migration rather than proliferation following focal brain injury. Brain Res 1024(1–2): 193–202
58. Frisen J, Johansson CB, Torok C, Risling M, Lendahl U (1995) Rapid, widespread, and longlasting induction of nestin contributes to the generation of glial scar tissue after CNS injury. J Cell Biol 131(2):453–464
59. Barnabe-Heider F, Goritz C, Sabelstrom H, Takebayashi H, Pfrieger FW, Meletis K, Frisen J (2010) Origin of new glial cells in intact and injured adult spinal cord. Cell Stem Cell 7(4):470–482
60. Meletis K, Barnabe-Heider F, Carlen M, Evergren E, Tomilin N, Shupliakov O, Frisen J (2008) Spinal cord injury reveals multilineage differentiation of ependymal cells. PLoS Biol 6(7), e182
61. Busch SA, Silver J (2007) The role of extracellular matrix in CNS regeneration. Curr Opin Neurobiol 17(1):120–127
62. Silver J, Miller JH (2004) Regeneration beyond the glial scar. Nat Rev Neurosci 5(2):146–156
63. Rohl C, Lucius R, Sievers J (2007) The effect of activated microglia on astrogliosis parameters in astrocyte cultures. Brain Res 1129(1): 43–52
64. Lacy M, Jones J, Whittemore SR, Haviland DL, Wetsel RA, Barnum SR (1995) Expression of the receptors for the C5a anaphylatoxin, interleukin-8 and FMLP by human astrocytes and microglia. J Neuroimmunol 61(1):71–78
65. Nakamura M, Okada S, Toyama Y, Okano H (2005) Role of IL-6 in spinal cord injury in a mouse model. Clin Rev Allergy Immunol 28(3):197–204
66. Norris JG, Tang LP, Sparacio SM, Benveniste EN (1994) Signal transduction pathways mediating astrocyte IL-6 induction by IL-1 beta and tumor necrosis factor-alpha. J Immunol 152(2):841–850
67. Sawada M, Itoh Y, Suzumura A, Marunouchi T (1993) Expression of cytokine receptors in cultured neuronal and glial cells. Neurosci Lett 160(2):131–134
68. Brunello AG, Weissenberger J, Kappeler A, Vallan C, Peters M, Rose-John S, Weis J (2000) Astrocytic alterations in interleukin-6/

Soluble interleukin-6 receptor alpha double-transgenic mice. Am J Pathol 157(5):1485–1493

69. Klein MA, Moller JC, Jones LL, Bluethmann H, Kreutzberg GW, Raivich G (1997) Impaired neuroglial activation in interleukin-6 deficient mice. Glia 19(3):227–233
70. Song Y, Zeng Z, Jin C, Zhang J, Ding B, Zhang F (2013) Protective effect of ginkgolide B against acute spinal cord injury in rats and its correlation with the JAK/STAT signaling pathway. Neurochem Res 38(3):610–619
71. Martinez FO, Gordon S (2014) The M1 and M2 paradigm of macrophage activation: time for reassessment. F1000Prime Rep 6:13
72. Benveniste EN (1998) Cytokine actions in the central nervous system. Cytokine Growth Factor Rev 9(3–4):259–275